

Aggregation-Induced Emission
How to cite: *Angew. Chem. Int. Ed.* **2020**, 59, 14903–14909

International Edition: doi.org/10.1002/anie.202004318

German Edition: doi.org/10.1002/ange.202004318

Direct Observation of Aggregation-Induced Emission Mechanism

Jianxin Guan⁺, Rong Wei⁺, Antonio Prlj⁺, Jie Peng, Kun-Han Lin, Jitian Liu, Han Han, Clémence Corminboeuf,* Dahui Zhao,* Zhihao Yu, and Junrong Zheng*

Dedicated to Professor Youqi Tang on the occasion of his 100th birthday

Abstract: The mechanism of aggregation-induced emission, which overcomes the common aggregation-caused quenching problem in organic optoelectronics, is revealed by monitoring the real time structural evolution and dynamics of electronic excited state with frequency and polarization resolved ultrafast UV/IR spectroscopy and theoretical calculations. The formation of Woodward–Hoffmann cyclic intermediates upon ultraviolet excitation is observed in dilute solutions of tetraphenylethylene and its derivatives but not in their respective solid. The ultrafast cyclization provides an efficient nonradiative relaxation pathway through crossing a conical intersection. Without such a reaction mechanism, the electronic excitation is preserved in the molecular solids and the molecule fluoresces efficiently, aided by the very slow intermolecular charge and energy transfers due to the well separated molecular packing arrangement. The mechanisms can be general for tuning the properties of chromophores in different phases for various important applications.

Introduction

In nature, most luminescent molecules glow strongly in dilute solutions but dimly in aggregate states. This phenomenon is well known as aggregation-caused quenching (ACQ).^[1] In many practical applications, for example organic or polymer light-emitting diodes, ACQ is a major limiting factor.^[2] In sharp contrast, a small group of molecules behave oppositely. The more molecules aggregate, the stronger their luminescence is.^[3] The aggregation-induced emission (AIE) phenomenon, in particular of molecules packed with bulky aromatic rings^[3c,4] owing to their structural similarity to many important optoelectronic molecules, has been considered as

an intriguing direction to overcome the problem of ACQ, which may open new doors for organic molecules in optoelectronic applications.^[5]

AIE and solidification-induced emission (SIE) are drawing tremendous research interest from both experiments and theory for the past 19 years^[5,6] but have a history of over 100 years,^[3c,7] however, their mechanisms are not fully disclosed. Long before the AIE concept was booming in the 2000 s, the nonradiative decay of excited tetraphenylethylene (TPE), a classical textbook AIE and SIE molecule, and its derivatives in solution was portrayed in terms of E–Z photoisomerization,^[8] borrowing the concepts, for example, of sudden polarization, phantom state etc., from the excited state dynamics of well-studied ethylene and stilbene molecules. The importance of torsional motion^[9] was also pointed out, for instance the systematic studies of tethered TPEs suggested that the phenyl ring torsions play a major role in deactivation of the excited singlet state, as opposed to traditionally assumed “olefinic twist” around the central double bond.^[10]

With the rise of the AIE field about twenty years ago, for typical AIE and SIE molecules with bulky aromatic rings like TPE, it has been generally proposed that the nonradiative decay in solution occurs due to the unhindered intramolecular rotations and vibrations, which serve as the energy acceptors for the electronic excitation energy.^[11] Restriction of intramolecular rotations (RIR)^[11] and vibrations (RIV)^[12] in aggregates, leading to the disappearance of these energy acceptors^[11] so that the electronic excitation energy is preserved, are responsible for AIE. The possibility of E–Z photoisomerization in solution has been considered as well, but its significance was ruled out.^[13]



However, the situation has changed over the last several years. There has been a series of experimental studies suggesting that the E–Z photoisomerization channel is the dominant deactivation channel in solution-based TPE.^[6b,c,14] Nevertheless, the direct observation of E–Z isomerization in solution is deemed as experimentally difficult.^[4b] As for the solid state and aggregate, induced emission can be explained by the steric restriction of the isomerization process.^[14a] Thus, the latest resolution of the dilemma between intramolecular phenyl rotation and E–Z isomerization, which was recently reviewed,^[4b] seems to favor the latter mechanism.

Despite the seemingly consensus being achieved, there has been a “third” mechanism which has been ignored in most of the literature, namely the photocyclization.^[15] Theoretical studies have proposed,^[6n] that after photoexcitation the structure of the electronic excited state of the molecule evolves and reaches a special point at which the electronic

[*] J. Guan,^[†] R. Wei,^[†] J. Peng, J. Liu, H. Han, Prof. D. Zhao, Prof. Z. Yu, Prof. J. Zheng
 College of Chemistry and Molecular Engineering, Beijing National Laboratory for Molecular Sciences, Peking University
 Beijing 100871 (China)
 E-mail: dhzhao@pku.edu.cn
 junrong@pku.edu.cn

A. Prlj,^[†] K.-H. Lin, Prof. C. Corminboeuf
 Laboratory for Computational Molecular Design, École polytechnique fédérale de Lausanne
 Lausanne (Switzerland)
 E-mail: Clémence.Corminboeuf@epfl.ch

[†] These authors contributed equally to this work.

 Supporting information and the ORCID identification number(s) for the author(s) of this article can be found under:
 <https://doi.org/10.1002/anie.202004318>.

excited state and an electronic ground state with highly excited vibrations are degenerated. At the geometry of conical intersection (CI),^[16] that is, the degeneracy between electronic states of the same multiplicity, the electronic excited state turns into the electronic ground state resonantly, so no emission occurs. Following the conversion, the electronic energy becomes mostly vibrational energy, and the highly excited vibrations of the electronic ground state rapidly dissipate their energy to other intra- and inter- molecular vibrations and rotations within hundreds of femtoseconds to picoseconds.^[17] In case of TPE, upon passing the CI, the molecule converts to a Woodward–Hoffmann type cyclic intermediate (or alternatively deactivates back to the original ground state structure, for example, via photoisomerization pathway). During this process, although the unhindered intramolecular rotations and vibrations are necessary for the fast nonradiative decay, they are not the energy acceptors. Instead, they provide the degrees of freedom for the electronic-excited molecule to isomerize to a particular structure. Upon aggregation, because of the imposed spatial and motional restrictions, the energy barrier to reach the conical intersection is too high for this nonradiative decay pathway to beat the emission channel. The electronic excitation is preserved and the molecule fluoresces. However, this mechanism is plagued, as the real-time structures evolving from the electronic excited state to the ground state in the dilute solution and the aggregate state are still elusive from experimental observations.

Results and Discussion

Real-Time Observations of Excited State Structural Evolution and Dynamics via Ultrafast UV/IR Spectroscopy

In this work, combining molecular designs, theoretical calculations, and frequency and polarization resolved ultra-violet/infrared (UV/IR) mixed frequency ultrafast spectroscopy, we are able to observe the structural evolution crossing the conical intersection in AIE molecules in real time, shedding light on the origins of the AIE phenomenon in TPE-type molecules.

Figure 1 displays the molecular structures of a typical AIE molecule tetraphenylethylene (TPE) and its cyclic isomer diphenyl dihydrophenanthrene (DPDHP) and the ultrafast UV/IR spectra at different waiting times of TPE solid. In Figure 1b, the *x*-axis is the excitation wavelength in the UV region from 280 to 360 nm and the *y*-axis is the detection frequency in the IR range from 2900 to 3150 cm^{-1} . Upon UV radiation, the TPE molecule is excited to the electronic excited state and its electronic and nuclear motions begin to evolve. The electronic excitation and the evolution of molecular motions lead to the appearance of vibrational peaks. Comparing spectra with different excitation wavelengths, for example, 290 nm and 330 nm in Figure 1c, we notice that, within experimental uncertainty, varying the excitation wavelength changes the intensity of the signal, but barely changes the major feature C–H stretch frequencies between 3000 cm^{-1} and 3100 cm^{-1} . Therefore, in the following, only a signal with excitation at 290 nm which is close to the UV absorption center (Figure S1 in the Supporting Information) is presented. More discussions about the signal/noise ratio and excitation wavelength independence are provided in the Supporting Information (Figure S14–S16).

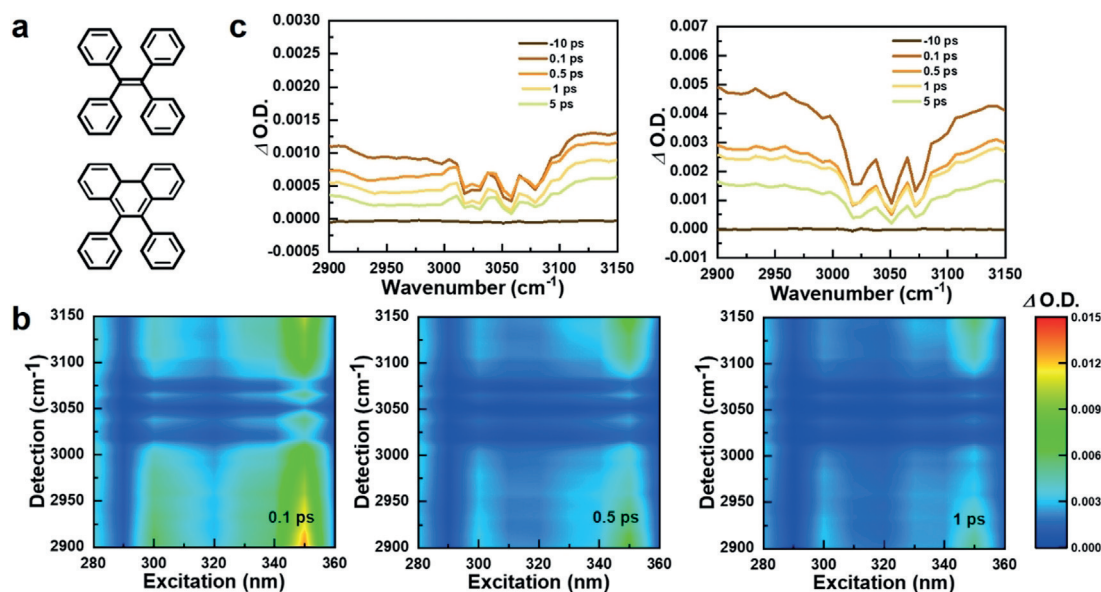


Figure 1. Structure of the typical AIE molecule tetraphenylethylene (TPE) and its cyclized isomer (diphenyl dihydrophenanthrene) as well as ultrafast UV/IR spectra in the TPE solid state. a) Molecular structure of TPE and DPDHP. b) Ultrafast UV/IR spectra at waiting times of 0.1 ps, 0.5 ps, and 1 ps, respectively. O.D., Optical Density. The spectra are not normalized with the excitation intensity. c) Spectra with excitation at 290 nm and 330 nm, respectively. The data are collected with the magic angle configuration.

Cyclization Process in TPE Solution

Figure 2a,b display the evolution of vibrational spectra of TPE in the solid state and in a dilute THF solution after excitation with light of 290 nm. In the solid sample, two absorption peaks appear at 1486 cm^{-1} and 1437 cm^{-1} upon UV excitation (Figure 2a). The peaks reach maxima almost instantaneously within the temporal resolution (about 100 femtoseconds) and diminish quickly. After 10 ps, their intensities have dropped by more than 70% (Figure 2c). These two peaks slightly redshift, compared to their respective peaks at 1489 cm^{-1} and 1442 cm^{-1} in the FTIR spectrum (Figure 2e), resulting from the excited state absorptions of the benzene skeleton vibration modes and frequency shifts induced by the electronic excitation.^[18] Accordingly, two corresponding small bleaching peaks grow in at their respec-

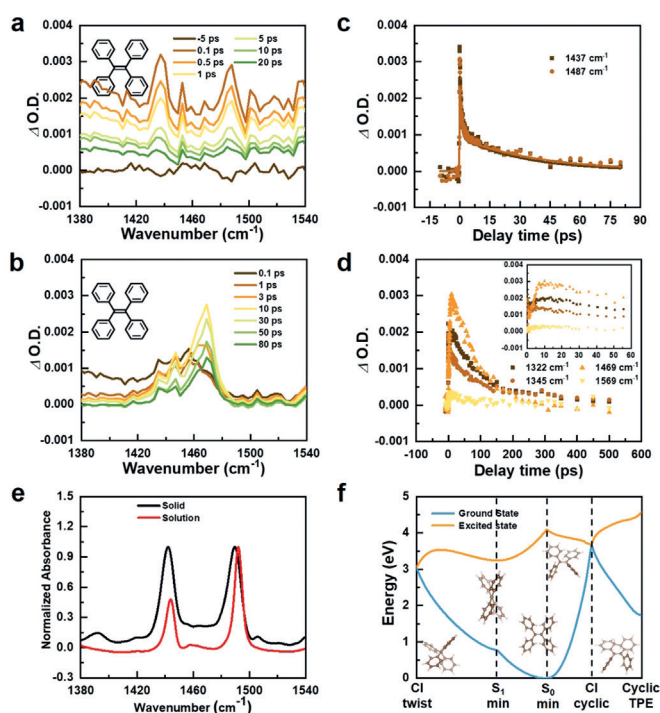


Figure 2. Dynamics and energy profile of TPE after excitation with a wavelength of 290 nm. Evolution of vibrational spectra of TPE (a) in the solid state and (b) in a dilute (50 mM) THF solution after excitation with photons at 290 nm. Signal decays of (c) the solid sample and (d) the THF solution detected at different IR frequencies. The signals reach maxima at time zero in the solid sample, whereas much slower at about 10 ps in the THF solution (insert in (d)). The peaks at 1322 , 1345 , and 1569 cm^{-1} are reported in Figure S5. e) FTIR spectra of TPE in solid state (black) and THF solution (red). The frequencies of the two major peaks are very similar, in contrast to the huge difference observed in the transient spectra in (a) and (b). The major feature of the transient spectra of the solid sample in (a) resembles that of FTIR spectra, distinctly different from that of the solution in (b). f) Computed energy profile of TPE after electronic excitation. The excited TPE molecule can deactivate by the Woodward–Hoffmann excited state cyclization (to the right), or by the *cis*–*trans* isomerization by twisting around the central ethylene bond (to the left). (a) to (b) are rotation-free data ($P(t) = (P_{\parallel}(t) + 2P_{\perp}(t))/3$). Data measured with both parallel and perpendicular polarizations are presented in Figure S3–S6 in the Supporting Information.

tive 0–1 transition frequencies, appearing at slightly blue-shifted 1497 cm^{-1} and 1447 cm^{-1} because of peak overlaps. The positive background of the signals in Figure 2a is probably caused by the absorption of weakly bound carriers generated by the UV excitation. Similar observations have been reported for organic materials.^[19]

In the dilute solution, despite its FTIR spectrum is very similar to the solid (Figure 2e), its ultrafast spectral evolution is distinctively different from the solid (Figure 2b). Upon UV excitation, a new absorption peak at 1469 cm^{-1} (Figure 2b) grows in, as well as peaks at 1322 , 1345 , and 1569 cm^{-1} (Figure S5), and at 3031 cm^{-1} , 3058 cm^{-1} and 3086 cm^{-1} (Figure S7). It reaches a maximum at around 10 ps (Figure 2b,d). Signals at early waiting times contain contributions from the solvent nonresonant response which decays much faster than the TPE signal (see Figure S8). In general, three possible mechanisms can lead to the appearance of these new peaks: the electronic excitation induced frequency shifts and vibrational excitations (coherent coupling), the energy conversion and transfer because of electron/vibration coupling, and the formation of new molecular structures initiated by photoexcitation, for example, ultrafast deactivation through the CI crossing.^[20] Since the signals of vibrational excitations or frequency shifts caused by electronic excitation are required to reach maxima upon excitation by the Frank–Condon principle^[21] as those in the solid sample, they are not the cause of these new peaks of which the maximum arrives several picoseconds after excitation. The energy conversion and transfer because of electron/vibration coupling is not the reason either, because none of the vibrational modes of TPE has the same frequencies as these new peaks in the transient spectra. Therefore, the appearances of these peaks indicate the formation of a new molecular structure. In other words, the system in solution crosses a conical intersection and reaches a new electronic ground state. In fact, these peaks are the characteristic vibrational signals of the long-anticipated new ground state, the theoretically predicted cyclic intermediate (Figure 2f, Figure S5, S7, S10, and Table S1 in the Supporting Information).

Our theoretical studies provide an interesting hint to possible pathways of the dynamics. Upon photoexcitation, the central C=C double bond reduces its bond order, and akin to the photoexcited ethylene molecule acquires a charge-resonance (S_1 min) character.^[8d,22] The excited state dynamics follows twisting motion around the central bond, until the conical intersection with a ground state is met. The *cis*–*trans* isomerization along the central C=C can occur, but due to the symmetric structure of TPE, the original ground state structure is restored after the isomerization. However, due to the presence of conjugated phenyl substituents, another competing mechanism of excited state deactivation may play a key role. The Woodward–Hoffmann excited state cyclization involving six carbon atoms may proceed, forming a covalent bond between the carbons of two neighboring phenyl rings. Figure 2f displays the computed excited state energy profile of TPE. Comparing the two possible pathways, the photocyclization appears as a barrierless process which requires a smaller reorganization of nuclear degrees of freedom (yellow line in Figure 2f from S_0 min to the yellow/

blue crossing point on the right). While the isomerization seems energetically more favorable, it requires large changes in nuclear coordinates, including the relaxation to the shallow S_1 minimum and crossing a small barrier to reach the conical intersection of twist configuration (yellow line in Figure 2 f from S_0 min to the left). Although it is likely that both mechanisms coexist together, our simulations^[15b] showed that the cyclization process dominates. This prediction is confirmed by the experimental results in Figure 2b. As discussed above, at very early waiting times before any dynamic event occurs, for example, 0 ps, the absorption peaks in Figure 2b are from the photoexcitation-induced frequency shifts and therefore their intensities can be used to represent the number of photo-excited molecules. In Figure 2b, the absorption peak at 1435 cm^{-1} at early waiting times, similar to that at 1437 cm^{-1} in Figure 2a of the solid sample, is caused by the photoexcitation-induced frequency shift of the benzene skeleton vibration mode. At 0.1 ps, the intensity of this peak with background subtraction is similar to that at 1469 cm^{-1} , indicating that a substantial number of photo-excited molecules have converted into the cyclic structure. At 10 ps, the peak at 1469 cm^{-1} is significantly larger than that at 1435 cm^{-1} . If the vibrational transition dipole moment of the peak at 1469 cm^{-1} is assumed to be similar to that of the peak at 1490 cm^{-1} of TPE, the sum of the two peaks at 1435 cm^{-1} and 1469 cm^{-1} at 0.1 ps normalized with the square of transition dipole moment ratio (roughly 1:2) can approximately represent the number of photo-excited molecules when most of them have not been deactivated. The percentage of initially photo-excited molecules converted into the cyclic structure at 10 ps can then be estimated by the normalized ratio between the peak at 1469 cm^{-1} and this sum. The results show that over 80 % of the excited molecules have been converted into the cyclic intermediate within 10 ps. This estimation is approximate, as spectral overlaps, the noise level (0.00005–0.0002), and the uncertain actual values of transition dipole moments can add uncertainties to the result. Nevertheless, the semi-quantitative evaluation suggests that a substantial number (probably over 50 %) of the photo-excited molecules have become the cyclic intermediate within 10 ps. A similar conclusion can be drawn from analyzing data of a TPE CH_2Cl_2 solution (Figure S7) that has a different solvent background at around 1450 cm^{-1} .

In our calculations, the cyclization process is barrierless for isolated molecules. However, in solutions, the formation of a cyclic intermediate involves many nuclear motions of the bulky rings which requires the reorganization of solvation structures. Therefore, its completion takes time and is dependent on solvation effects. As displayed in Figure 2d, it takes about 10 ps in THF for the signal to reach its maximum, and about 7–8 ps in CCl_4 (Figure S7). The cyclic intermediate is significantly less stable than the TPE electronic ground state (Figure 2 f). Under ambient condition, it can transform back into TPE, upon photoexcitation or thermal molecular collisions. As shown in Figure 2d, most of the cyclic intermediates last for only about 300 ps before they transform back to TPE. However, the lifetime is still sufficiently long for it to react with O_2 in the solution to form the cyclic product, which is isolated with HPLC and detected by MS (Figure S9).

The cyclization observed in TPE follows the Woodward–Hoffmann rules that predict a cyclization of excited 6- π -system that occurs via co-rotative torsion of conjugated moieties. The results are consistent with various previous experiments. For example, photocyclization has been reported experimentally as the first step in photo-oxidation of TPE to diphenyl-phenanthrene.^[22] The cyclic intermediate is known to be unstable, and if not trapped, it reverts back to the original compound.^[22c] *Cis*-stilbene (with two benzene rings of TPE replaced by two Hs) is known to undergo photocyclization in solution,^[23] though *trans*-stilbene is a prototype system for E–Z photoisomerization. It was estimated that up to 30 % of the excited state decay of *cis*-stilbene occurs via the cyclization channel,^[23b] which was well reproduced by the mixed quantum-classical simulations^[24] similar to those performed for TPE. It is reasonable that TPE, having two pairs of *cis*-phenyls, may undergo even more cyclization. Conversely, ethylenic twist with more bulky groups may be less favorable.

The different effects of UV excitation on the TPE dilute solution and solid sample can be understood from the standpoint of energy. In the dilute solution, the energy cost for the solvent molecules to adjust their configurations to accommodate the rotations and twisting of the benzene rings during the transformation of TPE to the cyclic intermediate is essentially the THF solvent molecule interaction energy, which is less than 1 kcal mol^{-1} .^[25] In the solid sample, the rotations and twisting of the benzene rings would require to break the crystalline structure. The energy cost is too high for it to be feasible.

The Formation of Cyclic Intermediates in Other AIE Molecular Solutions

Forming a cyclic intermediate is also observed in the other two solutions of AIE molecules **2** and **3**. The structures of these two molecules are displayed in the inserts of Figure 3 a,b. They also have four bulky groups connected to a C=C double bond. Once they are excited with UV light, they can transform into their respective cyclic intermediates. Their spectral evolutions after excitation with 290 nm light are shown in Figure 3 a,b. Similar to TPE, new vibrational absorption peaks appear at different frequencies which match reasonably well the theoretically predicted values of the cyclic intermediates (Figure S10 and Table S1). It is interesting that the time to reach the signal maximum is different for different molecules. For molecule **2**, it takes about 3.5 ps and for molecule **3** only 0.1 ps (Figure 3 e,f). The bulkier the side groups are, the faster the formation of the cyclic intermediate, as the initial configuration of the molecule with bulkier side groups is closer to that of the cyclic intermediate and larger side groups can hinder the competing twisting motion around the broken C=C bond. Similar to TPE, in the solid samples of these two molecules, the photoexcitation does not generate any new structures either. As displayed in Figure 3 c,d, only absorption and bleaching peaks caused by photo-excitation-induced vibrational excitations and frequency shifts appear.

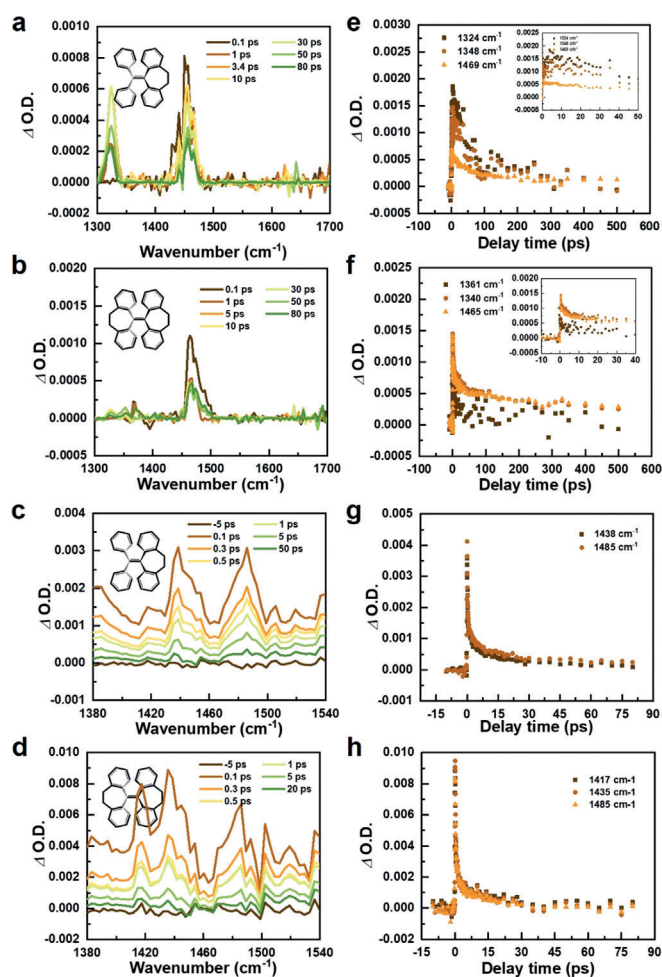


Figure 3. Transient vibration spectra and kinetics of molecule **2** and **3** after UV excitation. a–d) Transient vibrational spectra of molecule **2** (a) and **3** (b) in dilute THF solutions and in the solid state (c, d) after excited with light of 290 nm. e–h) Signal decays of molecule **2** and **3** in THF solutions (e, f) and in the solid state (g, h). Data are rotation-free.

Slow Process of Charge/Energy Transfers in AIE Molecular Solids

Lack of accessible conical intersection allows solids to preserve much more electronic energy needed for luminescence than it is the case in the dilute solutions. However, this is not sufficient for the AIE solids to avoid the quenching problem caused by charge or energy transfer that occurs in many other organic chromophores. There is another important feature of AIE molecules that allows them to significantly alleviate this problem and show relatively high luminescence quantum yields. The non-coplanar-oriented bulky side groups of AIE molecules prevent the excited electrons of one molecule from staying close to another molecule in the solid. Because of this repelling molecular stacking, the charge or energy transfer between molecules in closely-packed solids that usually cause quenching are difficult, in other words, very slow to proceed. The blocking of charge or energy transfer by molecular packing can be manifested with time dependent anisotropy measurements (Figure 4). Similar to energy transfer induced anisotropy

decay experiments,^[26] the anisotropy change in the present experiments reflects the charge or energy transfer in the solids. The initial anisotropy of our measurements is determined by the cross angle between the electronic transition and vibrational transition dipole moments within the same molecule. Following photoexcitation, if energy or charge transfers from the excited molecule to an adjacent molecule which typically has a different orientation, the anisotropy of the signal will change because after transfer it is determined by the cross angle between the electronic transition dipole moment of the donor molecule and the electronic/vibrational transition dipole moment of the acceptor molecule. As displayed in Figure 4, the anisotropy values of the ultrafast signals of AIE solids TPE, molecule **2**, and molecule **3** do not change up to 20 ps, unlike those of similar molecules with coplanar-oriented side groups, molecule **4** and **5**, for which the luminescence is quenched upon aggregation within a few ps. The results indicate that charge or energy transfer is very slow in the AIE solids, and the transfer occurs quickly in molecule **4** and molecule **5** where luminescence centers stack very close to each other.

Conclusion

In summary, photocyclization by crossing the conical intersection, a process which provides an efficient nonradiative relaxation pathway for electronic excitation and is too fast for conventional experimental tools, is observed in dilute solutions of AIE molecules TPE and its derivatives with ultrafast UV/IR spectroscopy. The inaccessibility of such crossings in solids helps to preserve electronic energy for luminescence. Large separation of luminescence centers among molecules in solids due to the non-coplanar packing effect of the bulky side groups significantly slows intermolecular charge and energy transfers and allows efficient luminescence. These two effects combined contribute to the abnormal AIE phenomenon. Crossing a CI is an ultrafast and efficient way to convert electronic excitation into heat (vibrations and rotations) and formation of new chemical bonds. A simple alteration of condition, for example, a liquid/solid phase transition in AIE, can turn it on or off and lead to dramatic changes in luminescence. Turning on/off the access to CI crossing is expected to be of practical importance for tuning the properties of chromophores in different phases in many applications, for example, sensing or displays, with various external stimuli (not limited only to phase transitions).

Acknowledgements

This material is based upon work supported by the National Science Foundation of China (NSFC-21627805, 21673004, 21821004, 21674001 and 21790363) and MOST (2017YFA0204702) China. We also acknowledge the support from the Construction Program of top technology discipline for colleges (Beijing) and the High-performance Computing Platform of Peking University for the computational resour-

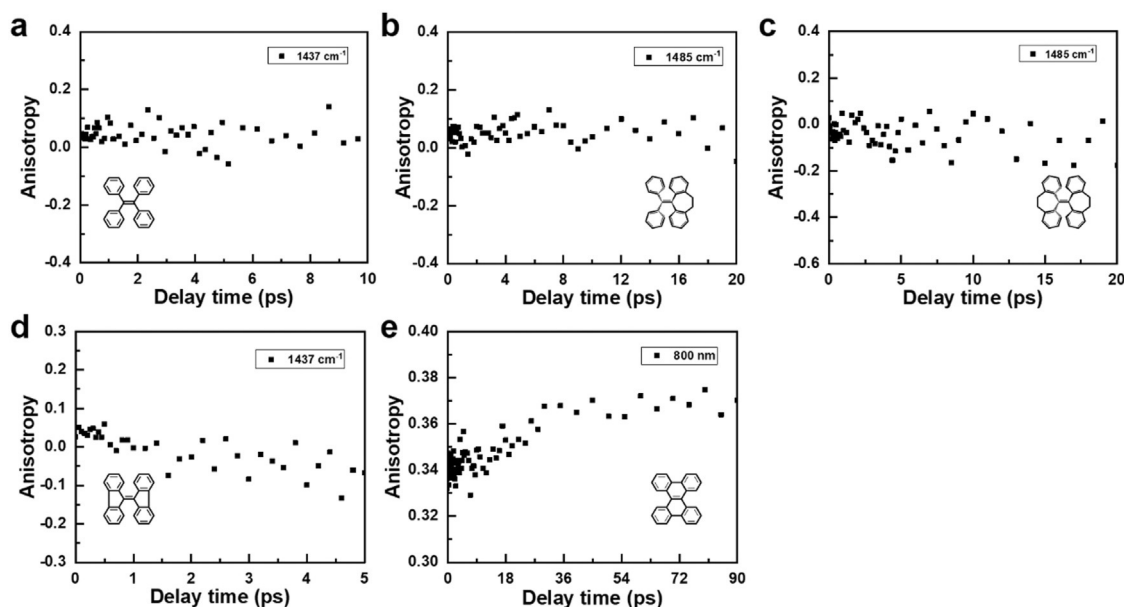


Figure 4. Time dependent anisotropy of UV/IR measurements. The Anisotropy value does not change for AIE molecules (a)–(c) whereas it changes within a few ps for ACQ molecules (d, e).

ces. A.P, K.H.L. and C.C. acknowledge EPFL for funding. Insightful discussion with Prof. Keith Nelson is deeply appreciated.

Conflict of interest

The authors declare no conflict of interest.

Keywords: aggregation-induced emission · conical intersections · luminescence · mechanism · ultrafast spectroscopy

- [1] J. Mei, N. L. Leung, R. T. Kwok, J. W. Lam, B. Z. Tang, *Chem. Rev.* **2015**, *115*, 11718–11940.
- [2] a) Y. Hong, J. W. Lam, B. Z. Tang, *Chem. Commun.* **2009**, 4332–4353; b) C.-C. A. Voll, J. U. Engelhart, M. Einzinger, M. A. Baldo, T. M. Swager, *Eur. J. Org. Chem.* **2017**, 4846–4851; c) K. Kawasumi, T. Wu, T. Zhu, H. S. Chae, T. Van Voorhis, M. A. Baldo, T. M. Swager, *J. Am. Chem. Soc.* **2015**, *137*, 11908–11911.
- [3] a) E. E. Jelley, *Nature* **1936**, *138*, 1009–1010; b) J. I. Zink, G. E. Hardy, J. E. Sutton, *J. Phys. Chem.* **1976**, *80*, 248–249; c) G. Fischer, E. Fischer, H. Stegemeyer, *Ber. Bunsen-Ges.* **1973**, *77*, 685–687.
- [4] a) J. Luo, Z. Xie, J. W. Y. Lam, L. Cheng, B. Z. Tang, H. Chen, C. Qiu, H. S. Kwok, X. Zhan, Y. Liu, D. Zhu, *Chem. Commun.* **2001**, 1740–1741; b) K. Kokado, K. Sada, *Angew. Chem. Int. Ed.* **2019**, *58*, 8632–8639; *Angew. Chem.* **2019**, *131*, 8724–8731.
- [5] a) F. Hu, S. Xu, B. Liu, *Adv. Mater.* **2018**, *30*, 1801350; b) D. Ding, C. C. Goh, G. Feng, Z. Zhao, J. Liu, R. Liu, N. Tomczak, J. Geng, B. Z. Tang, L. G. Ng, B. Liu, *Adv. Mater.* **2013**, *25*, 6083–6088; c) Y. Li, L. Xu, B. Su, *Chem. Commun.* **2012**, *48*, 4109–4111.
- [6] a) N. B. Shustova, T. C. Ong, A. F. Cozzolino, V. K. Michaelis, R. G. Griffin, M. Dinca, *J. Am. Chem. Soc.* **2012**, *134*, 15061–15070; b) Y. Cai, L. Du, K. Samedov, X. Gu, F. Qi, H. H. Y. Sung, B. O. Patrick, Z. Yan, X. Jiang, H. Zhang, J. W. Y. Lam, I. D. Williams, D. Lee Phillips, A. Qin, B. Z. Tang, *Chem. Sci.* **2018**, *9*, 4662–4670; c) J. B. Xiong, Y. X. Yuan, L. Wang, J. P. Sun, W. G. Qiao, H. C. Zhang, M. Duan, H. Han, S. Zhang, Y. S. Zheng, *Org. Lett.* **2018**, *20*, 373–376; d) J. Shi, N. Chang, C. Li, J. Mei, C. Deng, X. Luo, Z. Liu, Z. Bo, Y. Q. Dong, B. Z. Tang, *Chem. Commun.* **2012**, *48*, 10675–10677; e) N. L. Leung, N. Xie, W. Yuan, Y. Liu, Q. Wu, Q. Peng, Q. Miao, J. W. Lam, B. Z. Tang, *Chem. Eur. J.* **2014**, *20*, 15349–15353; f) B. Wang, X. Wang, W. Wang, F. Liu, *J. Phys. Chem. C* **2016**, *120*, 21850–21857; g) Y. Zhang, H. Mao, L. Kong, Y. Tian, Z. Tian, X. Zeng, J. Zhi, J. Shi, B. Tong, Y. Dong, *Dyes Pigm.* **2016**, *133*, 354–362; h) Z. Zhou, X. Yan, M. L. Saha, M. Zhang, M. Wang, X. Li, P. J. Stang, *J. Am. Chem. Soc.* **2016**, *138*, 13131–13134; i) M. Zhang, W. Yang, K. Li, W. Zhou, T. Gong, R. Xue, *Mater. Chem. Phys.* **2018**, *204*, 37–47; j) H. Tong, Y. Dong, Y. Hong, M. Häußler, J. W. Y. Lam, H. H. Y. Sung, X. Yu, J. Sun, I. D. Williams, H. S. Kwok, B. Z. Tang, *J. Phys. Chem. C* **2007**, *111*, 2287–2294; k) H. Gao, D. Xu, Y. Wang, Y. Wang, X. Liu, A. Han, C. Zhang, *Dyes Pigm.* **2018**, *150*, 59–66; l) Y. Liu, C. Deng, L. Tang, A. Qin, R. Hu, J. Z. Sun, B. Z. Tang, *J. Am. Chem. Soc.* **2011**, *133*, 660–663; m) H. Lu, Y. Zheng, X. Zhao, L. Wang, S. Ma, X. Han, B. Xu, W. Tian, H. Gao, *Angew. Chem. Int. Ed.* **2016**, *55*, 155–159; *Angew. Chem.* **2016**, *128*, 163–167; n) R. Crespo-Otero, Q. Li, L. Blancafort, *Chem. Asian J.* **2019**, *14*, 700–714.
- [7] a) J. Stark, P. Lipp, *Z. Phys. Chem.* **1913**, *86*, 36–41; b) G. C. Schmidt, *Ann. Phys.* **1921**, *370*, 247–256; c) G. Oster, Y. Nishijima, *J. Am. Chem. Soc.* **1956**, *78*, 1581–1584; d) S. Sharafy, K. A. Muszkat, *J. Am. Chem. Soc.* **1971**, *93*, 4119–4125.
- [8] a) J. Ma, G. B. Dutt, D. H. Waldeck, M. B. Zimmt, *J. Am. Chem. Soc.* **1994**, *116*, 10619–10629; b) B. I. Greene, *Chem. Phys. Lett.* **1981**, *79*, 51–53; c) E. Lenderink, K. Duppen, D. A. Wiersma, *J. Phys. Chem.* **1995**, *99*, 8972–8977; d) R. W. J. Zijlstra, P. T. van Duijnen, B. L. Feringa, T. Steffen, K. Duppen, D. A. Wiersma, *J. Phys. Chem. A* **1997**, *101*, 9828–9836.
- [9] P. F. Barbara, S. D. Rand, P. M. Rentzepis, *J. Am. Chem. Soc.* **1981**, *103*, 2156–2162.
- [10] a) D. A. Shultz, M. A. Fox, *Tetrahedron Lett.* **1988**, *29*, 4377–4380; b) D. A. Shultz, M. A. Fox, *J. Am. Chem. Soc.* **1989**, *111*, 6311–6320.
- [11] a) J. Zhao, D. Yang, Y. Zhao, X. J. Yang, Y. Y. Wang, B. Wu, *Angew. Chem. Int. Ed.* **2014**, *53*, 6632–6636; *Angew. Chem.* **2014**, *126*, 6750–6754; b) N. Sinha, L. Stegemann, T. T. Tan,

- N. L. Doltsinis, C. A. Strassert, F. E. Hahn, *Angew. Chem. Int. Ed.* **2017**, *56*, 2785–2789; *Angew. Chem.* **2017**, *129*, 2829–2833; c) J. W. Chen, C. C. W. Law, J. W. Y. Lam, Y. P. Dong, S. M. F. Lo, I. D. Williams, D. B. Zhu, B. Z. Tang, *Chem. Mater.* **2003**, *15*, 1535–1546.
- [12] a) J. Luo, K. Song, F. I. Gu, Q. Miao, *Chem. Sci.* **2011**, *2*, 2029–2034; b) S. Kumar, P. Singh, A. Mahajan, S. Kumar, *Org. Lett.* **2013**, *15*, 3400–3403.
- [13] Z. Yang, W. Qin, N. L. C. Leung, M. Arseneault, J. W. Y. Lam, G. Liang, H. H. Y. Sung, I. D. Williams, B. Z. Tang, *J. Mater. Chem. C* **2016**, *4*, 99–107.
- [14] a) K. Kokado, T. Machida, T. Iwasa, T. Taketsugu, K. Sada, *J. Phys. Chem. C* **2018**, *122*, 245–251; b) S. Kayal, K. Roy, S. Umapathy, *J. Chem. Phys.* **2018**, *148*, 024301.
- [15] a) A. Prlj, N. Doslic, C. Corminboeuf, *Phys. Chem. Chem. Phys.* **2016**, *18*, 11606–11609; b) T. Tran, A. Prlj, K. H. Lin, D. Hollas, C. Corminboeuf, *Phys. Chem. Chem. Phys.* **2019**, *21*, 9026–9035; c) Y.-J. Gao, X.-P. Chang, X.-Y. Liu, Q.-S. Li, G. Cui, W. Thiel, *J. Phys. Chem. A* **2017**, *121*, 2572–2579.
- [16] D. Y. W. Domcke, H. Köppel, *Advanced Series in Physical Chemistry, Vol. 17*, World Scientific, Singapore, **2011**, p. 768.
- [17] a) H. Chen, H. Bian, J. Li, X. Wen, Q. Zhang, W. Zhuang, J. Zheng, *J. Phys. Chem. B* **2015**, *119*, 4333–4349; b) I. V. Rubtsov, *Acc. Chem. Res.* **2009**, *42*, 1385–1394.
- [18] D. Xiao, M. Prémont-Schwarz, E. T. J. Nibbering, V. S. Batista, *J. Phys. Chem. A* **2012**, *116*, 2775–2790.
- [19] a) L. W. Barbour, M. Hegadorn, J. B. Asbury, *J. Am. Chem. Soc.* **2007**, *129*, 15884–15894; b) C. X. Sheng, M. Tong, S. Singh, Z. V. Vardeny, *Phys. Rev. B* **2007**, *75*, 085206.
- [20] Q. Li, L. Blancafort, *Chem. Commun.* **2013**, *49*, 5966–5968.
- [21] J. R. Lakowicz, *Principles of fluorescence spectroscopy*, Springer Science & Business Media, Cham, **2013**.
- [22] a) F. B. Mallory, C. S. Wood, J. T. Gordon, *J. Am. Chem. Soc.* **1964**, *86*, 3094–3102; b) R. J. Olsen, R. E. Buckles, *J. Photochem.* **1979**, *10*, 215–220; c) M. P. Aldred, C. Li, M. Q. Zhu, *Chem. Eur. J.* **2012**, *18*, 16037–16045; d) G. Huang, B. Ma, J. Chen, Q. Peng, G. Zhang, Q. Fan, D. Zhang, *Chem. Eur. J.* **2012**, *18*, 3886–3892; e) A. Jain, A. Achari, N. Mothi, M. Eswaramoorthy, S. J. George, *Chem. Sci.* **2015**, *6*, 6334–6340.
- [23] a) J. M. Rodier, A. B. Myers, *J. Am. Chem. Soc.* **1993**, *115*, 10791–10795; b) H. Petek, K. Yoshihara, Y. Fujiwara, Z. Lin, J. H. Penn, J. H. Frederick, *J. Phys. Chem.* **1990**, *94*, 7539–7543.
- [24] Y. Harabuchi, K. Keipert, F. Zahariev, T. Taketsugu, M. S. Gordon, *J. Phys. Chem. A* **2014**, *118*, 11987–11998.
- [25] J. Zheng, M. D. Fayer, *J. Am. Chem. Soc.* **2007**, *129*, 4328–4335.
- [26] a) K. P. Ghiggino, J. N. H. Reek, M. J. Crossley, A. W. Bosman, A. P. H. J. Schenning, E. W. Meijer, *J. Phys. Chem. B* **2000**, *104*, 2596–2606; b) H. Chen, X. Wen, X. Guo, J. Zheng, *Phys. Chem. Chem. Phys.* **2014**, *16*, 13995–14014; c) H. Bian, J. Li, X. Wen, J. Zheng, *J. Chem. Phys.* **2010**, *132*, 184505; d) H. Bian, X. Wen, J. Li, J. Zheng, *J. Chem. Phys.* **2010**, *133*, 034505.

Manuscript received: March 24, 2020

Revised manuscript received: May 3, 2020

Accepted manuscript online: May 22, 2020

Version of record online: June 22, 2020